

# Intrauterine Injection of Umbilical Cord Mesenchymal Stem Cell Exosome Gel Significantly Improves the Pregnancy Rate in Thin Endometrium Rats

Cell Transplantation  
Volume 31: 1–20  
© The Author(s) 2022  
Article reuse guidelines:  
sagepub.com/journals-permissions  
DOI: 10.1177/09636897221133345  
journals.sagepub.com/home/ct  
**SAGE**

Shengning Zhang<sup>1,2</sup>, Dongmei Wang<sup>2</sup>, Fang Yang<sup>1</sup>,  
YanJun Shen<sup>1</sup>, Dong Li<sup>3</sup> , and Xiaohui Deng<sup>1</sup> 

## Abstract

Human umbilical cord mesenchymal stem cell (HUMSC)-exosome gel played a significant role in promoting thin endometrial receptivity and improving the pregnancy rate by inhibiting endometrial fibrosis and accelerating subendometrial microangiogenesis. High-quality HUMSC-exosome were obtained by pretreating HUMSC with transforming growth factor- $\beta_1$  (TGF- $\beta_1$ ). Exosome gel mixture has good biocompatibility and physical rheological properties, stabilizing the structure of exosomes and prolonging the action of exosomes in the uterine cavity. HUMSC or HUMSC-derived exosomes were used to treat rat model of thin endometrium. In animal experiments, four groups, including the HUMSC, HUMSC-exosome, model (negative control), and sham operation groups, were designed. The therapeutic effects were evaluated by the thickness of the endometrium, the number of glands, the subendometrial vessel density, the markers of endometrial receptivity, and the pregnancy rate. In an *in vivo* study, three groups, involving HUMSC-coculture, HUMSC-exosome, and the control, were explored. The proliferation and migration of the human endometrial stromal cells (HESCs) were further determined by cell scratch and 5-ethynyl-2'-deoxyuridine (EdU) assays. The protein expression of the TGF- $\beta_1$ /smad2/3 signaling pathway was determined by Western blot. After treatment, the thickness of the endometrium, the number of glands, and the subendometrial microangiogenesis were obviously increased, and the level of inhibition of endometrial fibrosis, molecular markers of endometrial receptivity, and the pregnancy rate were also significantly improved. HUMSC-exosome and HUMSC significantly promoted the migration and proliferation of HESCs. And it was confirmed that HUMSC-exosome were superior to HUMSC in inhibiting HESCs fibrosis through TGF- $\beta_1$ /smad2/3 signaling pathway at the protein expression level.

## Keywords

pregnancy rate, thin endometrium, human umbilical cord mesenchymal stem cell, exosomes and gel

## Introduction

With the rapid development of assisted reproductive technology, it is now possible to significantly increase the clinical pregnancy rate; however, approximately half of the embryos in the transfer cycle still fail to implant, and these processes are governed by endometrium receptivity and embryo quality<sup>1,2</sup>. Good endometrial receptivity, which plays an important role in embryo implantation, is the premise of embryo implantation. A sufficient endometrial thickness is necessary for pregnancy, but there is no consensus on the definition of thin endometrium. Some scholars have suggested that a thin endometrium is defined as not thick enough to complete embryo implantation<sup>3</sup>. Moreover, subendometrial blood flow has been proposed as an important aspect of evaluating the receptivity of the endometrium<sup>4</sup>.

<sup>1</sup> Center for Reproductive Medicine, Department of Obstetrics and Gynecology, Qilu Hospital of Shandong University, Jinan, P.R. China

<sup>2</sup> Reproductive Medicine Center, Yantai Hospital, Yantai, P.R. China

<sup>3</sup> Cryomedicine Lab, Qilu Hospital of Shandong University, Jinan, P.R. China

Submitted: June 7, 2022. Revised: September 18, 2022. Accepted: September 29, 2022.

### Corresponding Authors:

Xiaohui Deng, Center for Reproductive Medicine, Department of Obstetrics and Gynecology, Qilu Hospital of Shandong University, Jinan 250012, Shandong Province, P.R. China.

Email: dxh250012@126.com

Dong Li, Cryomedicine Lab, Qilu Hospital of Shandong University, Jinan 250012, Shandong Province, P.R. China.

Email: lidong73@sdu.edu.cn



Recent research indicated that treatments using mesenchymal stem cell (MSCs) derived from bone marrow<sup>5,6</sup>, endometrium<sup>7,8</sup>, menstrual blood<sup>9</sup>, and the umbilical cord<sup>10</sup> could repair the damaged endometrium and promote tissue regeneration<sup>11–13</sup>. Furthermore, MSC secretion is now implicated as the primary mediator of MSC-based therapy. The secretory function includes cytokines and exosomes, among which the exosome contents are richer and more functionally defined, especially without DNA. Therefore, they have many advantages in the application of reproduction. Although MSC treatment is promising, limited survival after the implantation of biologically active agents in harsh environments is a bottleneck in disease treatment. Compared with stem cells, exosomes have many advantages<sup>14–17</sup>: (1) It is not necessary to consider issues of immune compatibility, tumorigenicity, embolism formation, or the transmission of infections; (2) They are easily stored without any loss of product potency; (3) It is more economical and practical for clinical applications when no invasive cell collection procedures are required; (4) Easily translated into mass production; and (5) MSC-exosome therapies can be immediately used for treatment.

Obtaining high-quality exosomes is the basis for improving the therapeutic effect. Various investigations have shown that the content of exosomes varies greatly. For example, the content of exosomes is different, and a single cell will also produce different types of exosomes under different conditions and growth stages<sup>18</sup>. The better the cellular state, the more the exosomes produced intrinsically by the cells. The mechanisms of exosome biogenesis and cargo-loaded cells should be explored further<sup>19</sup>. In addition to tissue fibrosis, transforming growth factor- $\beta_1$  (TGF- $\beta_1$ ) also regulates many biological responses, including cell proliferation, differentiation, autophagy, and immune response<sup>20</sup>. Therefore, we used TGF- $\beta_1$  to stimulate human umbilical cord mesenchymal stem cells (HUMSC) to improve the quality and purity of the exosomes. In this experiment, we used ethanol foam to establish a rat model of thin uterus, and then compared the therapeutic effects of MSC and MSC-exosome. The therapeutic effects were quantitatively evaluated by the thickness of the endometrium, the number of glands, the subendometrial vessel density, the markers of endometrial receptivity, and the pregnancy rate.

## Materials and Methods

### HUMSC Isolation, Culture, and Identification

Human umbilical cord samples were available from informed, consenting mothers and processed within the optimal period of 6 h. This experimental study was approved by the ethics committee of Qilu Hospital of Shandong University, China (No. 2018207). HUMSC were isolated from Wharton's jelly present in the umbilical cord by the tissue adherent method and were cultured in Dulbecco's modified Eagle medium/

nutrient mixture F12 (DMEM/F12) containing 10% fetal bovine serum (FBS; Gibco, Grand Island, USA) at 37°C in humidified air with 5% CO<sub>2</sub>. The identification method of the HUMSC is similar to that mentioned in Qi et al.<sup>21</sup>

To detect cell surface markers, the HUMSC were characterized for CD29, CD105, CD73, CD34, CD45, CD11b, CD44, and HLA-DR expression using flow cytometry according to the manufacturer's instructions. All antibodies used are listed in Table S2.

HUMSC ( $1 \times 10^6$ /well) were seeded in 6-well plates containing DMEM/F12 medium supplemented with 10% FBS. Osteogenic induction medium (0.1- $\mu$ M dexamethasone, 10-mM  $\beta$ -glycerol phosphate, and 50- $\mu$ g/ml ascorbic acid) was applied, and Alizarin red staining was performed 45 days after induction. Adipogenic differentiation medium (DMEM/F12 medium containing 100- $\mu$ M indomethacin, 10- $\mu$ M insulin, 1- $\mu$ M dexamethasone, and 0.5-mM 1-methyl-3-isobutylxanthine) was used for induction, and oil red O staining was performed 58 days after induction. Chondrogenic differentiation medium (Cyagen Biosciences) was employed for induction, fixation, embedding, sectioning, and Alcian blue staining after 3 weeks of induction. The HUMSC showed multilineage differentiation potential after being cultured in the respective induction medium.

### HUMSC-Exosome Pretreatment, Purification, and Identification

Based on our literature research and preexperiments, we used TGF- $\beta_1$  (10 ng/ml) to pretreat HUMSC to improve the output and quality of exosomes for 48 h. After 48 h, the culture supernatant was collected for HUMSC-exosome isolation. The exosomes were isolated following the procedure described in previous work<sup>22</sup>. The conditioned medium of the HUMSC was centrifuged at  $300 \times g$  for 10 min,  $2,000 \times g$  for 10 min, and  $10,000 \times g$  for 30 min to remove dead cells and cell debris, respectively. Then, the remaining supernatant was ultracentrifuged at  $100,000 \times g$  (Beckman Type 70 Ti, USA) for 70 min at 4°C. The pellet exosomes were suspended in 50- $\mu$ l phosphate-buffered saline (PBS) at -80°C for future experiments. The protein concentration of the concentrated exosomes was determined using a bicinchoninic acid (BCA) protein assay kit (Millipore, USA) according to the manufacturer's instructions.

**Transmission electron microscopy.** A drop of HUMSC-exosome suspension (20  $\mu$ l) was loaded onto formvar carbon-coated 200 mesh copper grids for 5 min at room temperature. Excessive fluid was removed with filter paper. Adsorbed exosomes were negatively stained with 3% (w/v) phosphotungstic acid (pH 6.8) for 5 min. After air-drying under an electric incandescent lamp, the sample was observed by transmission electron microscopy (TEM) (JEM-2100F; JEOL, Japan) operating at 100 kV. Randomized fields were captured, and



the exosomes in the field were counted by three independent researchers.

**Nanoparticle tracking analysis.** The number and size of the HUMSC-exosome were detected by nanoparticle tracking using ZetaView (Particle Metrix, Germany). The exosomes were diluted with PBS 1:1,000 to a final volume of 1 ml and loaded into a 1-ml syringe. The sample preparations were slowly injected into the sample chamber. After capture, the videos, recorded by using a CMOS camera and an embedded laser with a power of 40 mW and wavelength of 488 nm, were analyzed by built-in ZetaView Software 8.02.31.

**Western blot analysis of the protein expression of CD63, CD81, TSG101, and calnexin.** The HUMSC and exosome fractions were lysed in radioimmunoprecipitation assay (RIPA) lysis buffer with a protease inhibitor. The proteins were separated by sodium dodecyl sulfate–polyacrylamide gel electrophoresis and transferred onto a polyvinylidene difluoride (PVDF) membrane. The membrane was blocked in 5% milk for 1.5 h, and then exosome markers, including CD63, CD81, TSG101, and calnexin, were incubated with the primary antibodies overnight. Bands were incubated with goat anti-rabbit IgG (H+L) and horseradish peroxidase (HRP) conjugate. To assess the protein levels, the density of the bands in three independent experiments was quantified by ImageJ (V.1.8.0). All antibodies used are listed in Table S2.

**CCK-8 assay.** We used a CCK-8 kit (Beyotime Technology, China) to measure proliferation of human endometrial stromal cells (HESCs). Cells were seeded and cultured at a density of  $5 \times 10^3$ /well in 100  $\mu$ l of medium in 96-well plates. There are three groups: serum-free media group (control group), exosome group obtained by the traditional method (EXO group), and exosomes group obtained by TGF- $\beta_1$  optimization (EXO-TGF- $\beta_1$  group). At 1, 2, 3, 4, 5, and 6 days after the cells were treated with various medium, 10  $\mu$ l of CCK-8 reagent was added to each well and then cultured for 2 h. The absorbance was analyzed at 450 nm, and each experiment was repeated three times.

**Exosome labeling.** To identify the uptake of exosomes, exosomes were labeled with PKH26 fluorescent dye (Umibio Science and Technology Group, China), according to the manufacturer's protocol. Briefly, an appropriate amount of exosomes was taken for BCA protein concentration determination to determine the amount of exosomes. Separately, mix 50  $\mu$ l of diluent C with 5  $\mu$ l of PKH26. The exosome suspension was mixed with staining solution and incubated for 10 min. The labeling reaction was stopped by adding 10 ml of  $1 \times$  PBS. The labeled exosomes were centrifuged at  $100,000 \times g$  for 70 min to remove excess dye. Take 200  $\mu$ l of  $1 \times$  PBS to resuspend the pellet, which are the stained exosomes.

## Animal Model of Thin Endometrium Establishment and Treatment

Sprague–Dawley (SD) female rats between 7 and 9 weeks old weighing 150–200 g were selected as research targets in our experiments. The rats were housed in groups with free access to food and water and were maintained on a regular 12-h light/dark cycle. Vaginal cytology performed in the morning was used to obtain the frequency and regularity of the estrous cycle after 1–2 weeks of acclimatization. Forty rats with the same estrous cycles were selected for our research. All animal experiments were performed in strict accordance with the “National Institutes of Health Guide for the Care and Use of Laboratory Animals.” This study was reviewed and approved by the Institutional Review Board and the Ethics Committee of Qilu Hospital, Shang Dong University (No. DULL-2020-044).

Rats anesthetized with propofol (7.5 ml/kg) were placed in the supine position, and the inferior abdomen was shaved and disinfected with 70% ethanol and 2% chlorhexidine diacetate (Nolvasan®) solutions. After confirming adequate anesthesia by loss of toe-pinch reflexes, a transverse lower abdominal incision was made sharply and carried down to the peritoneal cavity. The uterine horns were identified and confirmed to have grossly normal anatomy. Ethanol foam was prepared by adding ethanol (48%), sorbitol ester 80 ( $5 \times 10^{-3}$  g/ml), and egg yolk lecithin ( $10^{-2}$  g/ml) mixtures to hyaluronic acid and rapidly injecting the mixture 30–40 times at room temperature through a 10-ml syringe<sup>23,24</sup>, and the effect was the same as that of absolute ethanol. The ethanol foam was injected into the uterine cavity via an intravenous catheter (BD Insyte™, 22G), and the time was recorded. When the uterus became pale, the injection was immediately stopped, and the uterine cavity was quickly flushed with normal saline. The right side was treated in the same way. After the operation, the rats were awakened in an incubator, and penicillin sodium was given to prevent infection. Rats were randomly divided into four groups: the model group (treated with PBS,  $n = 10$ ), HUMSC group (treated with HUMSC,  $2 \times 10^7$  cells/200  $\mu$ l/per uterine,  $n = 10$ ), HUMSC-exosome group (treated with HUMSC-exosome gel, 150–200  $\mu$ g/per uterine, 30 ml of the culture supernatant derived from  $2 \times 10^7$  cells, suspended in 200  $\mu$ l of gel,  $n = 10$ ), and the sham operation group (operation without modeling,  $n = 10$ ). During surgery, 20 min after modeling, we directly perfused the uterus cavity with an intravenous catheter. At 3 and 5 days after modeling, we infused the uterine cavity with vaginal infusion therapy. Exosomes are mixed with gel [MateRegen, BioRegen Biomedical (Changzhou) Co., Ltd., China], which are mainly composed of cross-linked sodium hyaluronate, sodium chloride, disodium hydrogen phosphate, sodium dihydrogen phosphate, and water for injection. To assess the condition of the endometrium, some rats were anesthetized for sampling at 4–5 estrous cycles after treatment ( $n = 5$ ).

### ***Hematoxylin and Eosin and Masson's Trichrome Staining***

The uterine tissues of rats were processed for paraffin embedding by slicing into 4- $\mu$ m sections. The sections were stained with hematoxylin and eosin (H&E) and Masson's trichrome according to standard protocols (Solarbio, Beijing Solarbio Science & Technology Co., Ltd.). Using the H&E staining images, the mean thickness of the endometrium was determined from four measurements at 0°, 90°, 180°, and 270° in horizontal sections, and the number of glands was counted on the horizontal sections by 40 $\times$  magnification. From images of tissues with Masson's trichrome staining, parameters were calculated using quantitative morphometry (ImageJ-Pro Plus).

### ***Immunohistochemical Staining***

Immunohistochemistry (IHC) was performed by following a standard protocol (ZSGB-BIO). Briefly, endogenous peroxidase was blocked with 3% hydrogen peroxidase after antigen retrieval. The specimens were blocked with 10% normal goat serum for 1 h. The expression of Pan-CK11, vimentin, CD34, and vascular endothelial growth factor A (VEGFA) proteins was determined by incubating rat uterine slides with rabbit polyclonal antibodies against Pan-CK11, vimentin, CD34, and VEGFA overnight at 4°C. The slides were incubated with secondary antibody dilution followed by DAB (Diaminobenzidine, ZLI-9018, ZSGB-BIO) solution for 1 h. Then, the cells were briefly stained with hematoxylin solution (15 s) and evaluated by a microscope (Nikon DS-Ri1-U3). All antibodies used are listed in Table S2.

### ***Immunofluorescent Staining***

Tissue sections were fixed with 4% paraformaldehyde, permeabilized with 0.3% Triton X-100, blocked with 1% bovine serum albumin (BSA), and subsequently stained with anti-leukemia inhibitory factor (LIF) primary antibodies (Table S2) overnight at 4°C. The appropriate fluorescent-conjugated secondary antibodies were used prior to nuclear staining with 4',6-diamidino-2-phenylindole (DAPI) solution and tracked by a microscope.

### ***Real-Time PCR***

Total RNA was extracted from the uterus of the rats by using an extraction reagent (TRIzol, Gibco), and the concentration was measured by a spectrophotometer. The isolated RNAs were reverse-transcribed by using a cDNA Synthesis Kit (Accurate Biology, USA) based on the provided protocol. Quantitative reverse transcription-polymerase chain reaction (qRT-PCR) was performed using a SYBR<sup>®</sup>-x0005-qRT-PCR

mix in a CFX96™ real-time system (Bio-Rad, USA). Glyceraldehyde 3-phosphate dehydrogenase (GAPDH) served as an internal control. The sham operation group was regarded as the control group, and its value was set to 1. All reactions were performed in triplicate. The quantitative expression level was analyzed using the 2- $\Delta\Delta$ Ct method. The primers used for qRT-PCR are listed in Table S1.

### ***Western Blotting to Test the Protein Expression of Endothelial Receptivity and Fibrosis***

Total protein was extracted from uterine tissues of rats or HESCs according to the protocol, and the protein content was detected using a BCA protein assay kit. All antibodies used are listed in Table S2. Mouse monoclonal anti-GAPDH was used as the internal control. The sham operation group was the control group.

### ***Fertility Testing***

All the rats were randomly assigned to the four groups: the sham operation group (n = 5), HUMSC group (n = 5), HUMSC-exosome group (n = 5), and model group (n = 5). All female rats were mated with male rats (1:1) at 4–5 estrus cycles after treatment, and the day when a vaginal plug was observed was considered successful mating. Rats in each group were euthanized after 10–14 days when the vaginal plug fell off, and the number and site of embryos in each group were recorded.

### ***In Vivo Tracing of HUMSC and HUMSC-Exosome Hydrogel***

After establishing the rat thin endometrium model, the HUMSC and their derived exosomes were labeled with red fluorescent dye PKH26 (Cat. No: PKH26PCL, Sigma-Aldrich) according to the instructions to trace the cells and exosomes, respectively. The HUMSC group was treated with HUMSC ( $2 \times 10^7$  cells/200  $\mu$ l/per uterine, n = 5) and the HUMSC-exosome group was treated with HUMSC-exosome gel (150–200  $\mu$ g/per uterine, n = 5). Subsequently, fluorescence images were acquired using an IVIS Spectrum imaging system (PerkinElmer, USA) at 24, 48, and 72 h after perfusion.

### ***Cell Scratch Assay***

HESCs were seeded in six-well plates ( $10^5$  cells/well). After 24 h, two straight lines were drawn on the plate with a pipette tip, and serum-free medium (control group), exosomes (HUMSC-exosome group), and HUMSC (HUMSC-coculture group) were added. Images of the scratched cells

were taken at 0 and 24 h using a microscope. The migration ability of the cells was analyzed based on the healed area of the scratch.

### EdU Staining Assay

HESCs were cultured in a 96-well plate and treated with 100  $\mu$ l of medium containing 20- $\mu$ M 5-ethynyl-2'-deoxyuridine (EdU) according to the following protocol (Alexa Fluor 555, BeyoClick™ EdU Cell Proliferation Kit, Biotime, Shanghai, China). After incubation at 37°C, with 5% CO<sub>2</sub> for 2 h, the cells were fixed with 4% paraformaldehyde for 15 min and incubated with 0.5% Triton X-100 in PBS for 15 min. The nuclei were stained with Hoechst dye 33342. EdU-positive cells were analyzed in different treatment groups.

### Statistical Analysis

The data in our study are presented as mean  $\pm$  standard deviation (SD). All experiments were performed independently, at least in triplicate. Student's *t* test was used for comparisons between two groups. For multiple group comparisons, one-way or two-way analysis of variance (ANOVA) with Tukey's post hoc test was used. Statistical significance with the threshold of *P* < 0.05, <0.01, or <0.001 was calculated by using GraphPad Prism 8 software (La Jolla, CA, USA).

## Results

### In Vitro Culture, Phenotypic Identification, and Induced Differentiation Ability of HUMSCs

The HUMSC obtained from human umbilical cord tissues were grown in culture. The cells crawled out of the umbilical cord tissue mass after 72 h. After 5–7 days, the cells became longer, closely attached to each other, and spread around. The growth rate increased rapidly when the cells grew to the third generation. We observed that the HUMSC included polygonal, swirling, and fibroblast-like cells (Fig. 1A). It seems that passage 3 of the HUMSC proliferated the fastest, as shown in their growth curve (Fig. 1B). Flow cytometry analysis indicated that CD29, CD73, CD105, and CD44 were positively expressed in HUMSC, whereas CD11b, CD34, CD45, and HLA-DR were negatively expressed (Fig. 1C). The results of induced differentiation experiments confirmed that the HUMSC could differentiate into adipogenic, osteogenic, and chondrogenic phenotypes (Fig. 1D). After osteogenic induction, positive alkaline phosphatase staining appeared. Fat droplets appeared after lipogenic induction and oil red O staining was positive. Chondrogenesis induction followed by Alcian blue staining shows blue deposits, demonstrating the presence of type II collagen deposition, a typical sign of chondrocytes.

### Typical Characteristics of HUMSC-Exosome and Significant Changes After Pretreatment With TGF- $\beta_1$

To obtain exosomes, we used gradient ultracentrifugation to extract the exosomes from the conditioned culture supernatants (Fig. 2A). Nanoparticle tracking analysis (NTA) showed that the particles contained a large number of HUMSC-derived vesicles with a diameter of 90–150 nm, and the peak of the curve was located at 103.7 nm (Fig. 2B). TEM suggested that the exosomes had a granular oval appearance. Due to the dehydration of the TEM sample during the preparation process, the surface of the exosomes was wrinkled (Fig. 2C). Our Western blot analysis confirmed that the vesicles expressed the exosome-specific protein markers CD81, CD63, TSG101, and calnexin (Fig. 2D). These observations indicated that the vesicles were HUMSC-derived exosomes. The concentration of exosomes after pretreatment with TGF- $\beta_1$  was significantly higher than that without TGF- $\beta_1$  (Fig. 2E). In the CCK-8 proliferation assay, the proliferation rate of HESCs in the EXO-TGF- $\beta_1$  group was significantly faster than that in the control group. Moreover, the EXO-TGF- $\beta_1$  group was the fastest among the three (Fig. 2F). The HUMSC-exosome had been absorbed and phagocytosed by HESCs (Fig. 2G).

### H&E and Masson's Trichrome Staining Changes in the Endometrium

The restoration of the thin endometrium following different treatments was assessed by H&E (Fig. 3A) and Masson's trichrome staining (Fig. 3B). After modeling, the endometrial layer became thinner, the endometrial glands became fewer, and the original intact structure was lost. In the other groups (HUMSC and HUMSC-exosome), the endometrial layer became thicker and the number of glands increased. In addition, the endometrial structure in the HUMSC and HUMSC-exosome groups was most similar to that in the sham operation group. From the H&E stained images, the endometrium could be seen to be severely damaged, glands and blood vessels were scarce, and severe endometrial thinning was apparent in the model group. Compared with the model group (25.263  $\pm$  0.501, 5.25  $\pm$  2.630), the HUMSC (131.605  $\pm$  22.528, 27.000  $\pm$  6.218) and HUMSC-exosome groups (148.407  $\pm$  38.803, 24.750  $\pm$  4.272) showed that the regenerated endometrium was significantly thicker (Fig. 3C, *P* < 0.0001 and <0.001, respectively) than that of the model group, and the number of glands was significantly increased (Fig. 3C, *P* < 0.001, respectively).

To evaluate collagen remodeling in the reconstructed endometrium after HUMSC or HUMSC-exosome therapy, Masson's trichrome staining was performed, and the areas of collagen staining were analyzed quantitatively. After



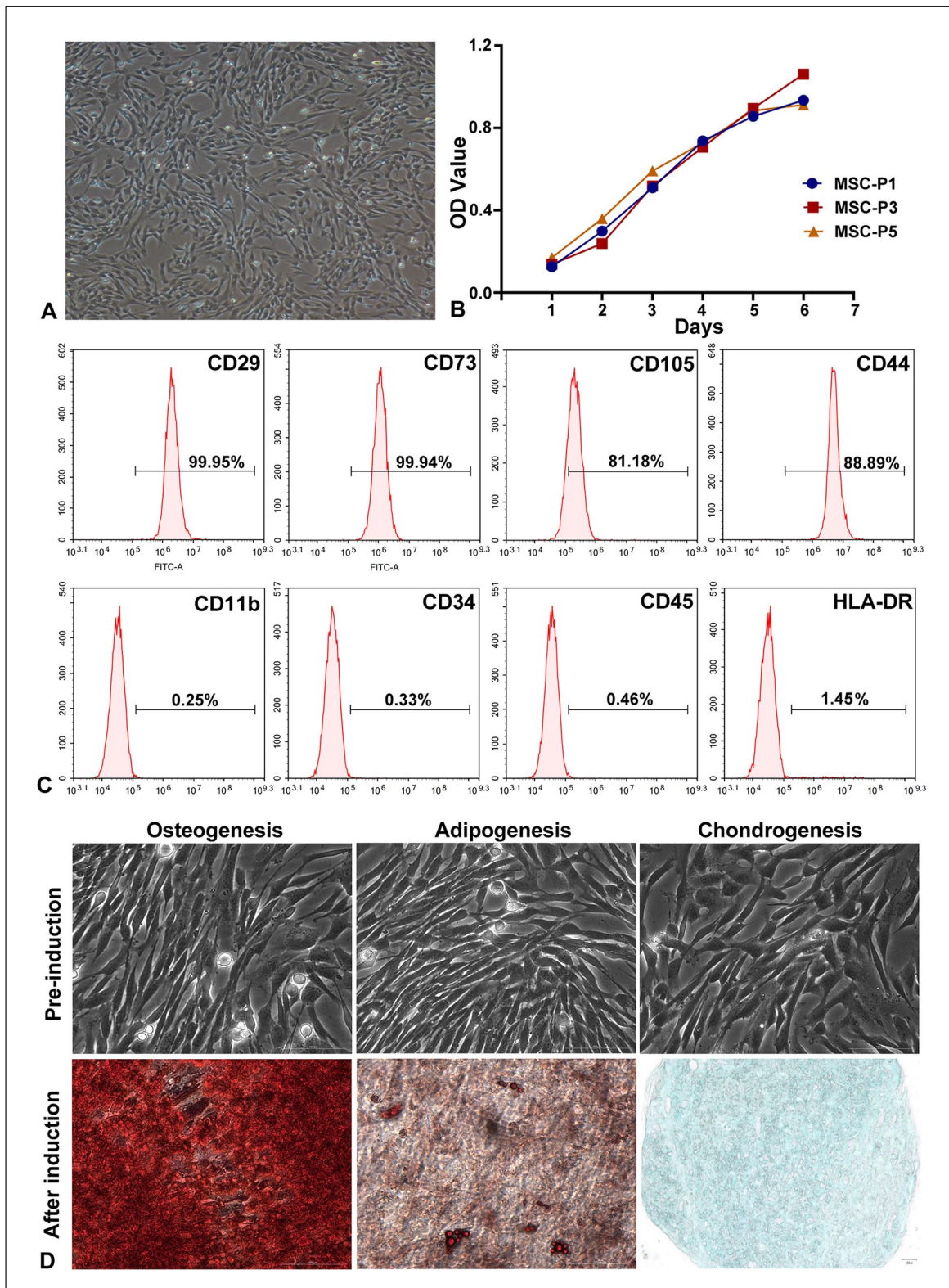


**Figure 1.** Isolation and identification of HUMSC. (A) The morphology of HUMSC passage 3. (B) The growth curve of passages 1, 3, and 5 of HUMSC. (C) Flow cytometry analysis of the surface phenotypes of the HUMSC. (D) Representative images of osteoporosis induction (200 $\times$ ), adipogenesis induction (200 $\times$ ), and chondrogenesis induction (400 $\times$ ). The cells were analyzed using cytochemical staining with Alizarin red, oil red O, and Alcian blue. Osteogenic induction, red was a positive signal; lipogenic induction, oil red O staining was positive; chondrogenesis induction, Alcian blue staining showed blue type II collagen deposits, blue was positive. HUMSC: human umbilical cord mesenchymal stem cell; MSC: mesenchymal stem cell.



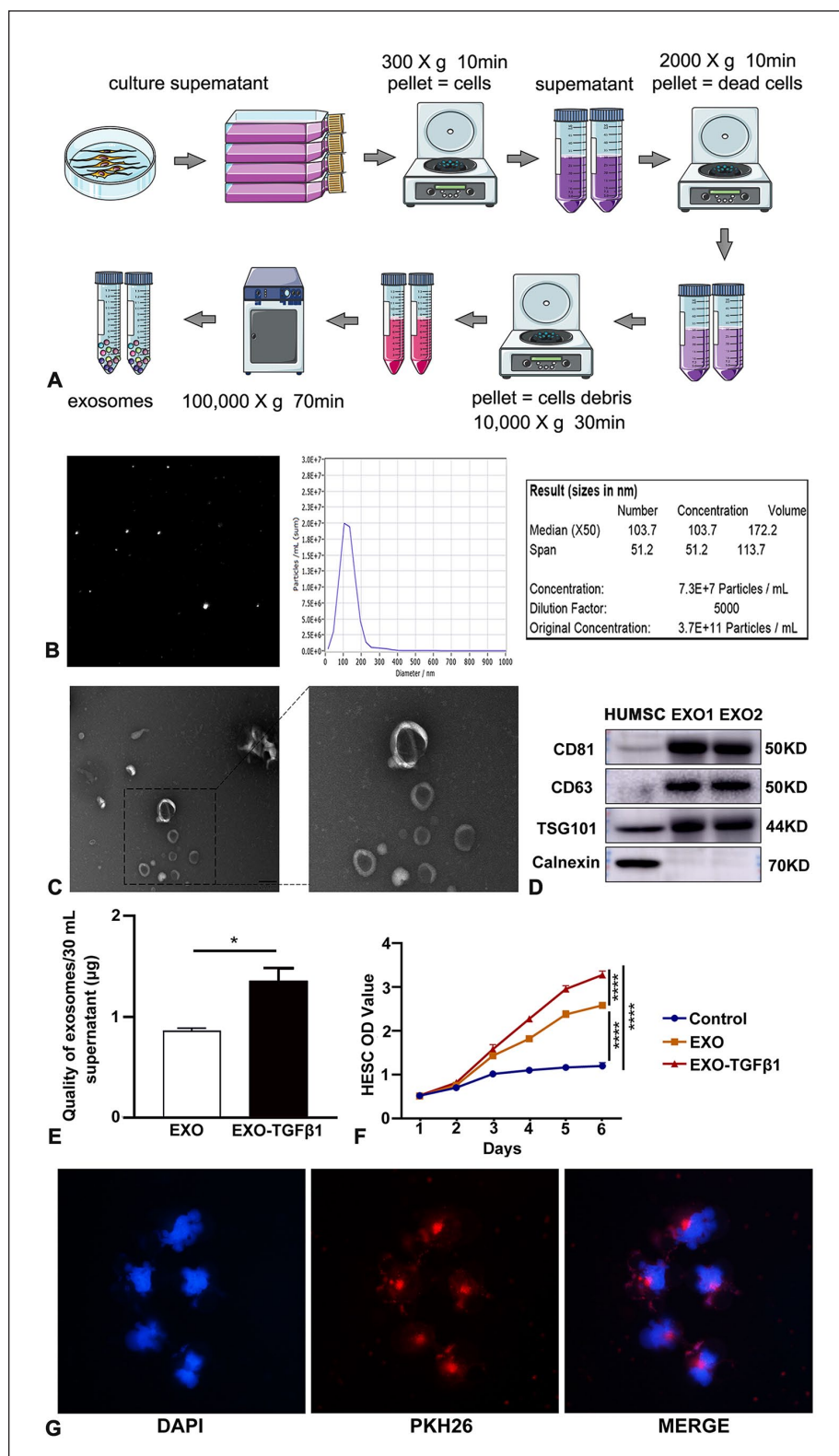


**Figure 2.** Identification of exosomes derived from HUMSC. (A) The HUMSC-exosome extraction procedure. (B) NTA of the HUMSC-exosome. (C) Transmission electron photomicrograph of the HUMSC-exosome. (D) CD81, CD63, TSG101, and calnexin expression in HUMSC-exosome detected by Western blot. (E) Protein concentration measured by the BCA method of the EXO-TGF- $\beta_1$  group (exosome pretreatment with TGF- $\beta_1$ ) and EXO group (exosomes without pretreatment). (F) CCK-8 growth curve of HESCs in the EXO-TGF- $\beta_1$  group, EXO group, and control group. (G) HUMSC-exosome were taken up and phagocytosed by HESCs. HUMSC: human umbilical cord mesenchymal stem cell; NTA: nanoparticle tracking analysis; BCA: bicinchoninic acid; EXO-TGF- $\beta_1$ : exosome group obtained by TGF- $\beta_1$  optimization; TGF- $\beta_1$ : transforming growth factor- $\beta_1$ ; HESCs: human endometrial stromal cells.

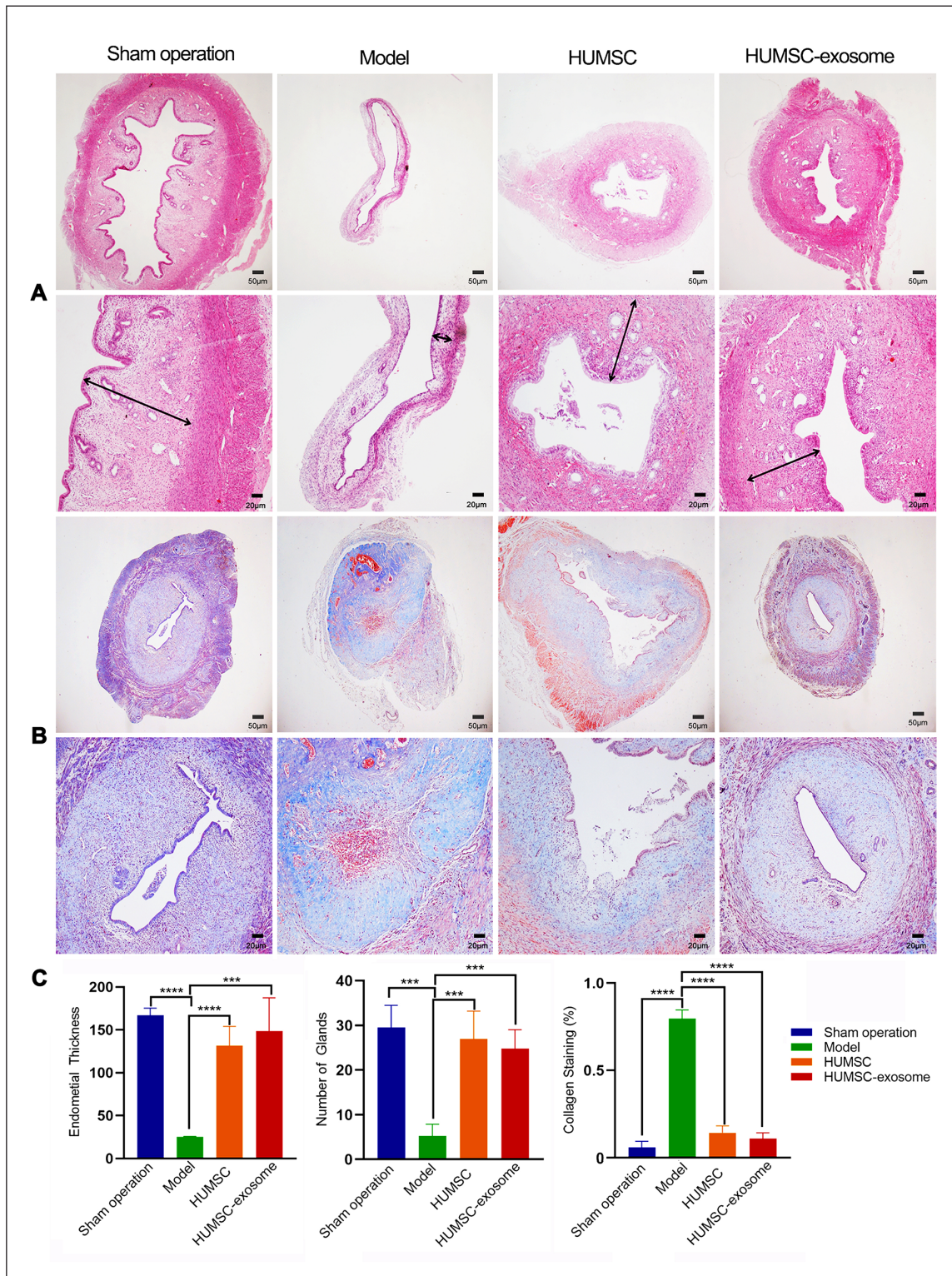


**Figure 3.** (A) H&E staining of the uterus of rats treated with HUMSC or HUMSC-exosome. The black arrows indicate the endometrial thickness. Scale bar: 50 μm (40×), 20 μm (100×). (B) Masson's trichrome staining of the uterus of rats treated with HUMSC or HUMSC-exosome. Scale bar: 50 μm (40×), 20 μm (100×). (C) Evaluating the treatment effect from three aspects: the thickness of the endometrium, the number of glands, and the area of collagen fibers. Data were presented as mean ± SD. H&E: hematoxylin and eosin; HUMSC: human umbilical cord mesenchymal stem cell. \*\*\* $P < 0.001$ ; \*\*\*\* $P < 0.0001$ , compared with the model group;  $n = 5$ .



modeling, the uterine cavity became narrow, and blood stasis appeared in the model group, whereas the symptoms of blood stasis were alleviated in the HUMSC or HUMSC-exosome groups. The histogram showed that the treatment groups (HUMSC/HUMSC-exosome) had lower collagen deposition than the model group (Fig. 3C,  $P < 0.0001$ , respectively).

### **Immunohistochemical Staining of Vimentin and Cytokeratin**

Vimentin (Fig. 4A) and cytokeratin (Fig. 4B) were expressed in the cytoplasm of the endometrial epithelial cells and stromal cells, respectively. Early rapid reepithelialization is critical for subsequent endometrial recovery after endometrial damage. Vimentin and cytokeratin are markers of endometrial recovery.

The number of vimentin-positive and cytokeratin-positive cells was increased in the HUMSC and HUMSC-exosome groups after treatment. After therapy, the HUMSC/HUMSC-exosome showed significant upregulation of the percentage of vimentin-positive (Fig. 4C,  $P < 0.001$  and  $<0.0001$ , respectively) and cytokeratin-positive (Fig. 4C,  $P < 0.001$ , respectively) areas compared with the model group.

### **Immunohistochemical Staining of VEGF and CD34**

Promoting microangiogenesis is an essential step in tissue repair; thus, VEGFA, a specific vascular endothelial cell growth-promoting factor, was assessed by IHC staining. After therapy, the number of VEGFA-positive cells in the HUMSC or HUMSC-exosome groups was significantly higher than that in the model group (Fig. 5A). The bar graph shows higher expression in the treatment groups (HUMSC/HUMSC-exosome) (Fig. 5C,  $P < 0.001$  and  $<0.05$ , respectively) than in the model group. To study the effects of HUMSC or HUMSC-exosome on promoting microvascular regeneration, we performed IHC staining for CD34 (Fig. 5B), which is a highly specific vascular endothelial marker. The results showed that the microvessel density (MVD) of the HUMSC and HUMSC-exosome groups was significantly higher than that of the model group (Fig. 5C,  $P < 0.01$ , respectively) and was similar to that of the sham operation group after therapy.

### **Immunofluorescence Staining of LIF**

LIF is crucial for the formation of the maternal decidua, which is produced by the endometrial glands and acts on the endometrial epithelium to make it receptive to blastocyst attachment and on the stroma to decidualise it for implantation and placental development<sup>25</sup>. Immunofluorescence

staining of LIF (red fluorescence) revealed that its protein expression was obviously high in the HUMSC and HUMSC-exosome groups and similar to the sham operation group but showed almost no expression in the model group (Fig. 6A). The results showed that the LIF fluorescence intensity of the HUMSC and HUMSC-exosome groups was significantly higher than that of the model group (Fig. 6B,  $P < 0.0001$ , respectively).

### **In Vivo Tracing of HUMSC and HUMSC-Derived Exosome Hydrogel After Intrauterine Injection**

To track HUMSC and HUMSC-exosome *in vivo*, HUMSC and exosomes were successfully labeled by PKH26 in accordance with the method depicted in the previous study. We investigated HUMSC and exosome-hydrogel retention and distribution at different time points using *in vivo* fluorescence imaging (Fig. 7A and C). Results showed that much stronger fluorescence was reserved at the damaged zone of HUMSC-exosome hydrogel than HUMSC for a long time *in vivo* in living rats (Fig. 7B,  $P < 0.01$ , respectively).

### **Recovery of Fertility in the Rat Model of Thin Endometrium After Therapy**

As shown in Fig. 8, we further evaluated whether HUMSC or HUMSC-exosome could improve pregnancy outcomes in a rat model of thin endometrium. All the rats in the sham operation group became pregnant (100%), while the pregnancy rates in the HUMSC group and HUMSC-exosome groups were 60% and 80%, respectively, which were higher than those in the model group ( $P < 0.0001$ ). The number of embryo implantations was highest in the sham operation group ( $n = 5$ ), with 13, 17, 15, 15, and 13 embryos, respectively, with no embryo implantation in the model group. Compared with the model group, the number of embryos implanted in the HUMSC group and HUMSC-exosome group was highly increased at 4, 9, 7, 0, 0; and 16, 18, 13, 5, 0 ( $P < 0.0001$  and  $<0.0001$ , respectively). There were more embryos in the HUMSC-exosome group than the HUMSC group, but the difference was not statistically significant.

### **qPCR and Western Blotting for the Expression of Endometrial Fibrosis-Related and Receptivity-Related Molecular Markers**

Quantitative PCR (qPCR) was applied to examine the expression of endometrial fibrosis-related and receptivity-related mRNAs after treatment. Endometrial fibrosis is considered to be an important pathological change in a thin endometrium. Factors related to fibrosis, such as TGF- $\beta_1$ , connective tissue growth factor (CTGF), plasminogen activator inhibitor 1 (PAI-1), and collagen I, were significantly

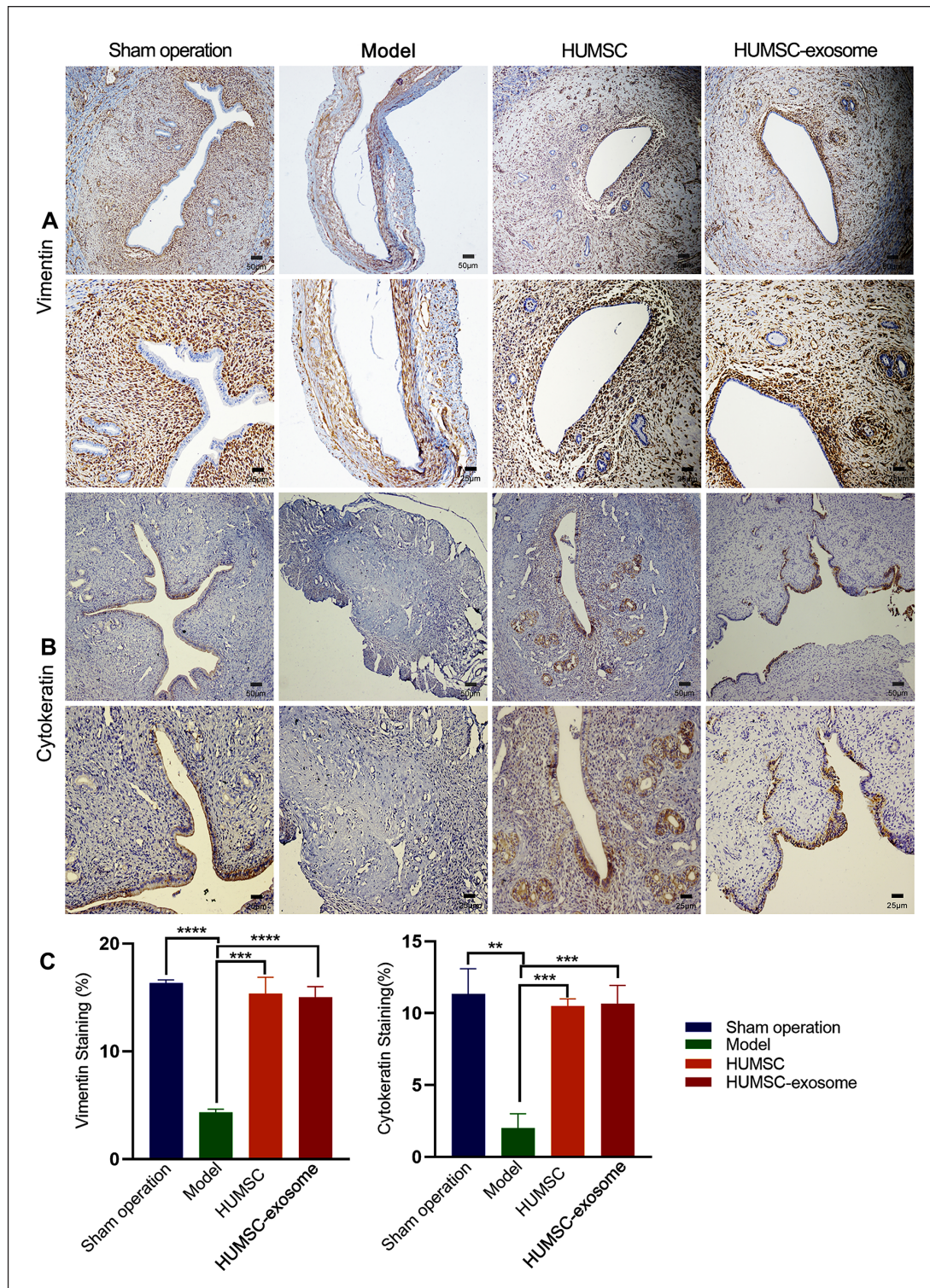


**Figure 4.** Effects of HUMSC and HUMSC-exosome therapy on endometrial epithelial and stromal cell proliferation. (A) Vimentin and (B) cytokeratin protein expression in each group was detected by IHC, where brown-yellow particles were deposited. Scale bar: 50  $\mu$ m (100 $\times$ ), 25  $\mu$ m (200 $\times$ ). (C) The histogram showed the endometrial vimentin and cytokeratin staining percentage of the rat endometrium in each group. Data were presented as mean  $\pm$  SD. HUMSC: human umbilical cord mesenchymal stem cell; IHC: Immunohistochemistry. \*\* $P < 0.01$ ; \*\*\* $P < 0.001$ ; \*\*\*\* $P < 0.0001$ , compared with the model group;  $n = 5$ .



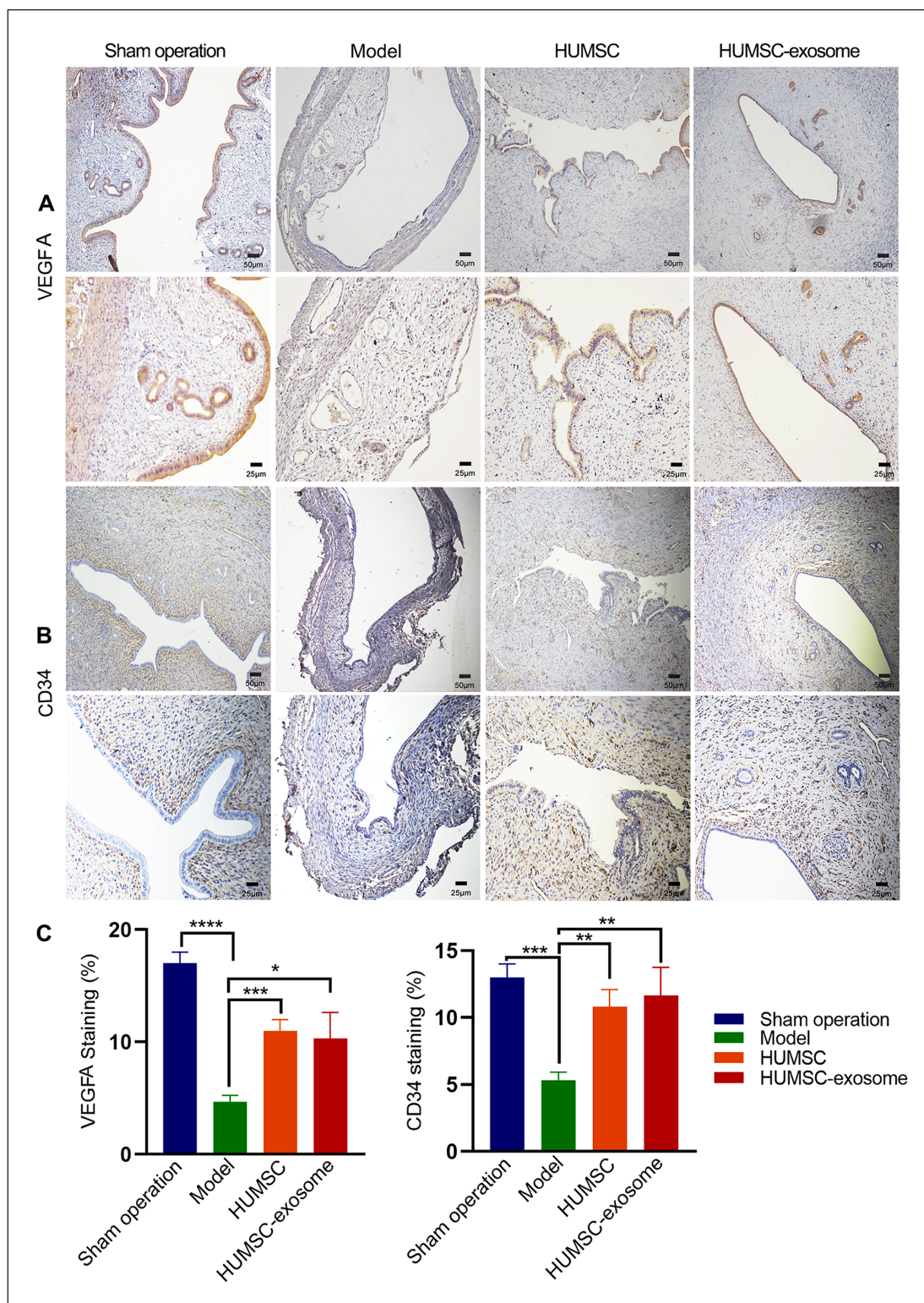


**Figure 5.** Effects of HUMSC and HUMSC-exosome therapy on promoting microangiogenesis. (A) VEGFA and (B) CD34 protein expression in each group was detected by IHC, where brown-yellow particles were deposited. Scale bar: 50  $\mu$ m (100 $\times$ ), 25  $\mu$ m (200 $\times$ ). (C) The histogram showed the endometrial VEGFA and CD34 staining percentage of the rat endometrium in each group. Data were presented as mean  $\pm$  SD. HUMSC: human umbilical cord mesenchymal stem cell; VEGFA: vascular endothelial growth factor A; IHC: immunohistochemistry. \* $P$  < 0.05; \*\* $P$  < 0.01; \*\*\* $P$  < 0.001; \*\*\*\* $P$  < 0.0001, compared with the model group;  $n$  = 5.



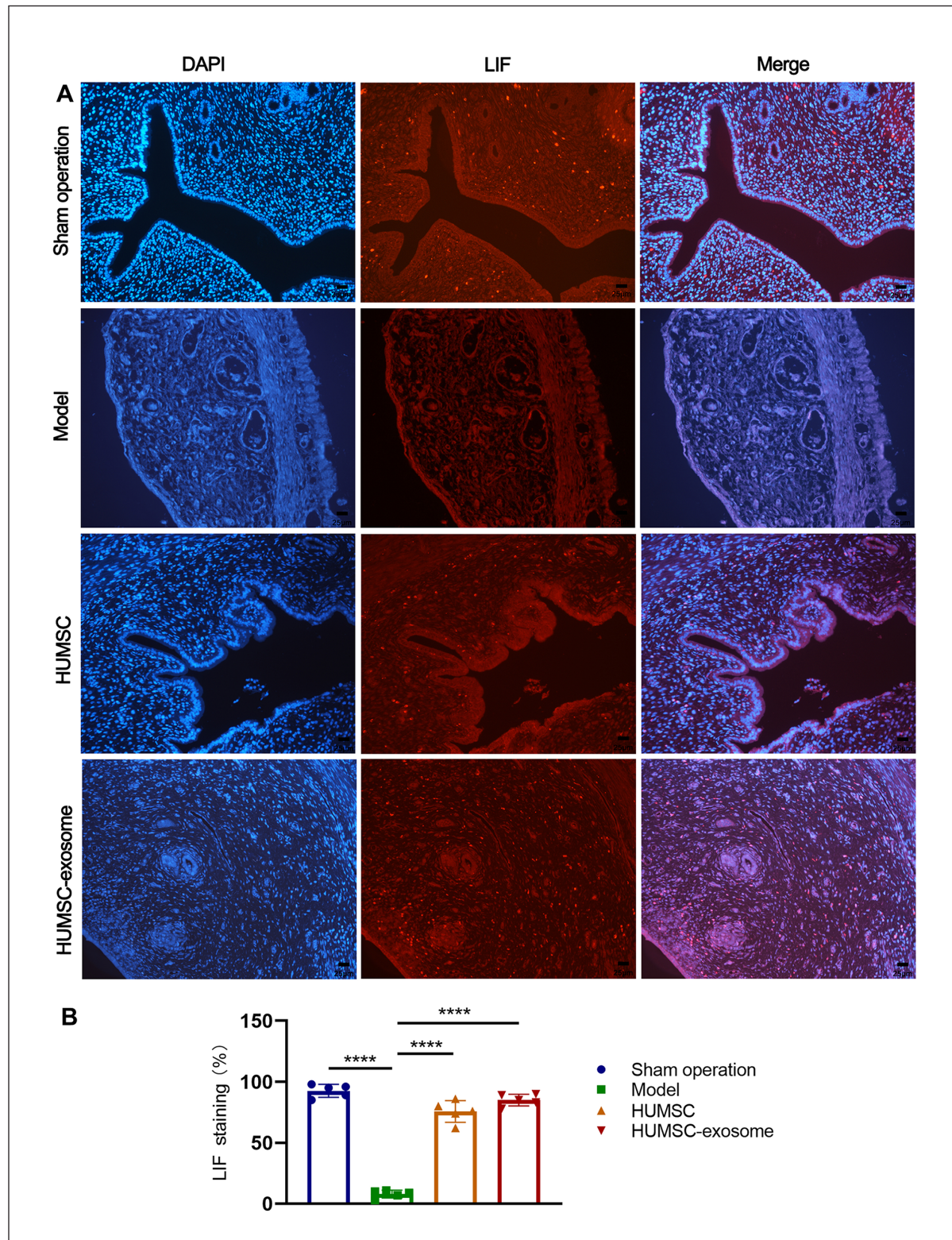


**Figure 6.** (A) Effects of HUMSC and HUMSC-exosome therapy on improving endometrial receptivity. LIF protein expression in each group was detected by immunofluorescent staining, and the red fluorescent represented the expression of LIF. (B) The histogram showed the endometrial LIF staining percentage of the rat endometrium in each group. Scale bar: 25  $\mu$ m (200 $\times$ ),  $n = 5$ . Data were presented as mean  $\pm$  SD. HUMSC: human umbilical cord mesenchymal stem cell; LIF: leukemia inhibitory factor; DAPI: 4',6-diamidino-2-phenylindole. \*\*\*\* $P < 0.0001$ , compared with the model group;  $n = 5$ .

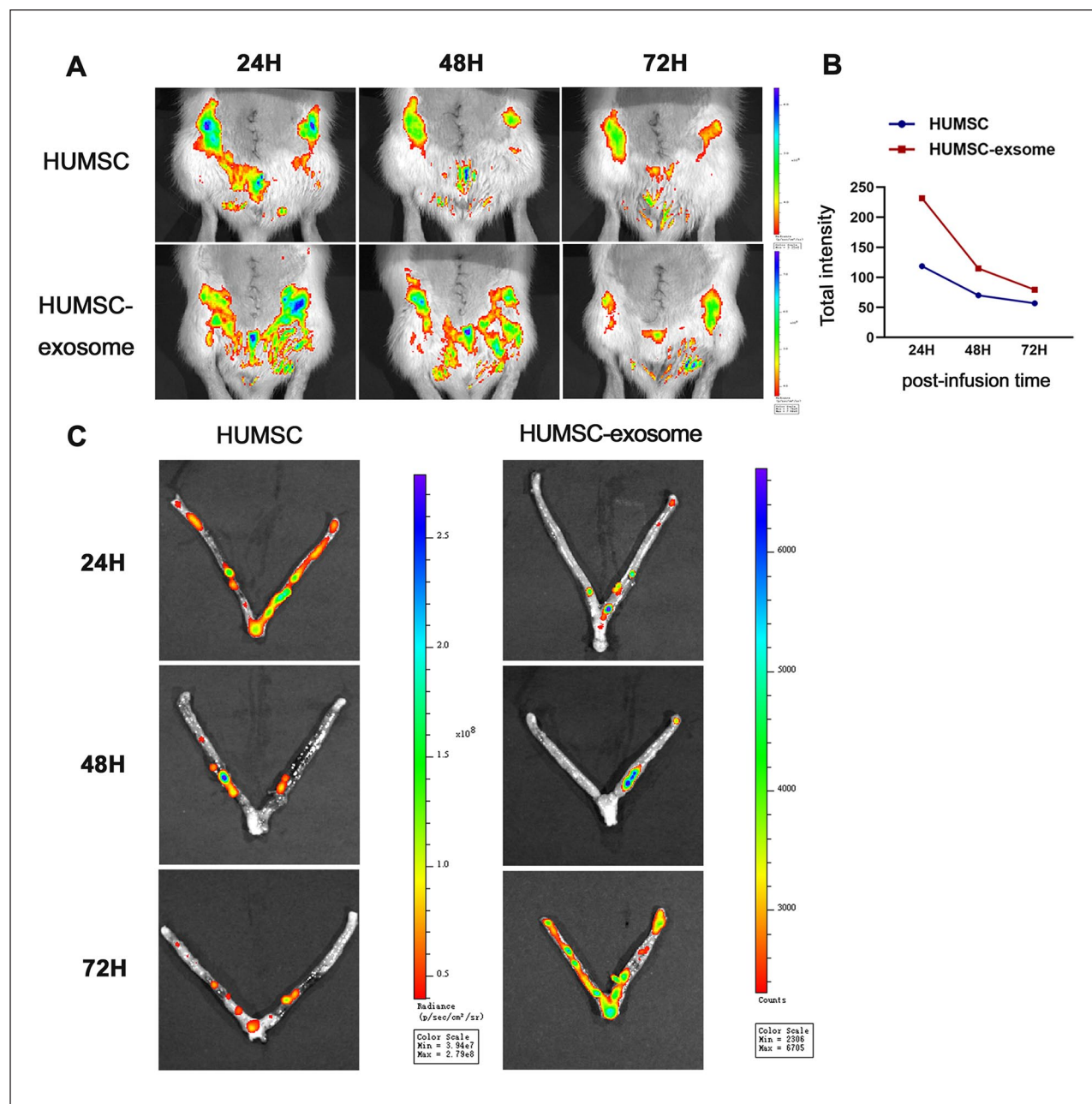


**Figure 7.** *In vivo* tracing of HUMSC and HUMSC-exosome hydrogel. Representative IVIS images of the retention of HUMSC or HUMSC-exosome at different time points after intrauterine injection in the thin endometrium model of rats *in vivo* or *in vitro* (A and C). Quantification of the fluorescence intensity in HUMSC group and HUMSC-exosome group after intrauterine injection *in vivo* in living rat model of thin endometrium (B). Data were presented as mean  $\pm$  SD. HUMSC: human umbilical cord mesenchymal stem cell.  $*p < 0.01$ , compared with the model group;  $n = 5$ .

decreased in the HUMSC, HUMSC-exosome, and sham operation groups compared with the model group (Fig. 9A). In contrast, the expression of VEGF and LIF related to endometrial receptivity in the HUMSC or HUMSC-exosome group was obviously higher than that in the model group (Fig. 9D). The tendency of Western blotting for the

expression of fibrosis markers was the same as the mRNA expression of TGF- $\beta_1$ , CTGF, PAI-1, and collagen I (Fig. 9B). Similarly, the protein expression levels of vimentin, cytokeratin, integrin  $\beta_3$ , LIF, and VEGF, associated with endometrial receptivity, were higher in the HUMSC and HUMSC-exosome group than in the model group (Fig. 9C).



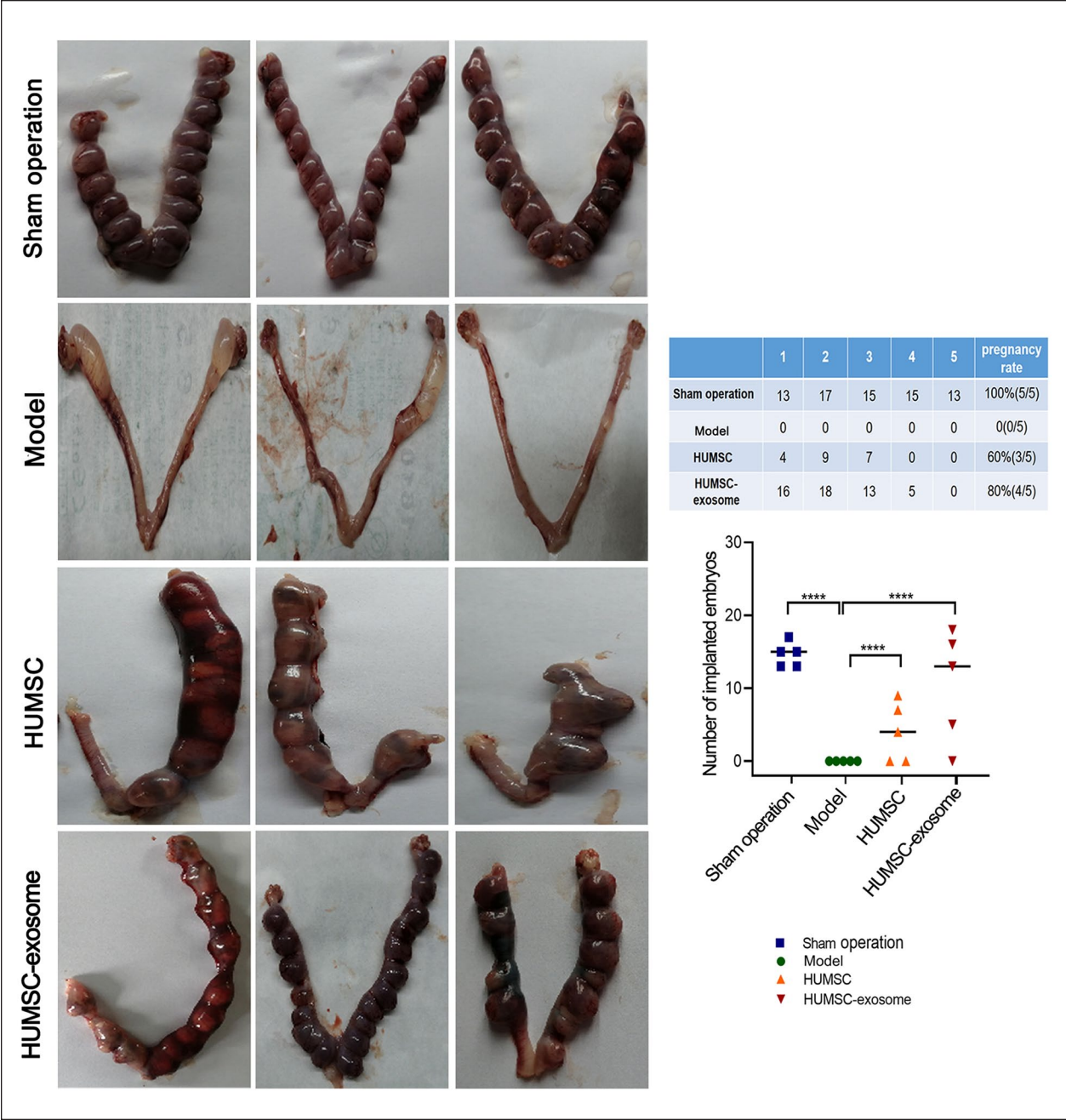


**Figure 8.** Effects of different treatments on fertility restoration. Picture displayed uterine embryo implantation of the rats in each group. Table showed pregnancy status and pregnancy rate in each treatment group. The scatter plot showed the embryo implantation ratio in the sham operation group, model group, HUMSC group, and HUMSC-exosome group. Bars represented mean  $\pm$  SD. HUMSC: human umbilical cord mesenchymal stem cell. \*\*\* $P < 0.0001$  versus the model group,  $n = 5$ .

*HUMSC and HUMSC-Exosome Attenuated Endometrial Fibrosis by Regulating TGF- $\beta_1$  to Inhibit the Phosphorylation of Smad2/3 and Promote the Migration and Proliferation of HESCs*

To verify the effects of HUMSC and HUMSC-exosome on HESCs, cell migration was analyzed by a cell scratch test. The results indicated that the migration potential of the

HUMSC group and HUMSC-exosome group was greater than that of the control group after 24 h ( $P < 0.0001$  and  $<0.0001$ , respectively) (Fig. 10A and B). To further confirm the effect of the proliferation on HESCs, EdU was used to detect DNA replication (green fluorescence) after culture in the HUMSC-exosome medium and the HUMSCs were cocultured with the HESCs for 24 h. The DNA replication of HESCs in the HUMSC group and HUMSC-exosome group



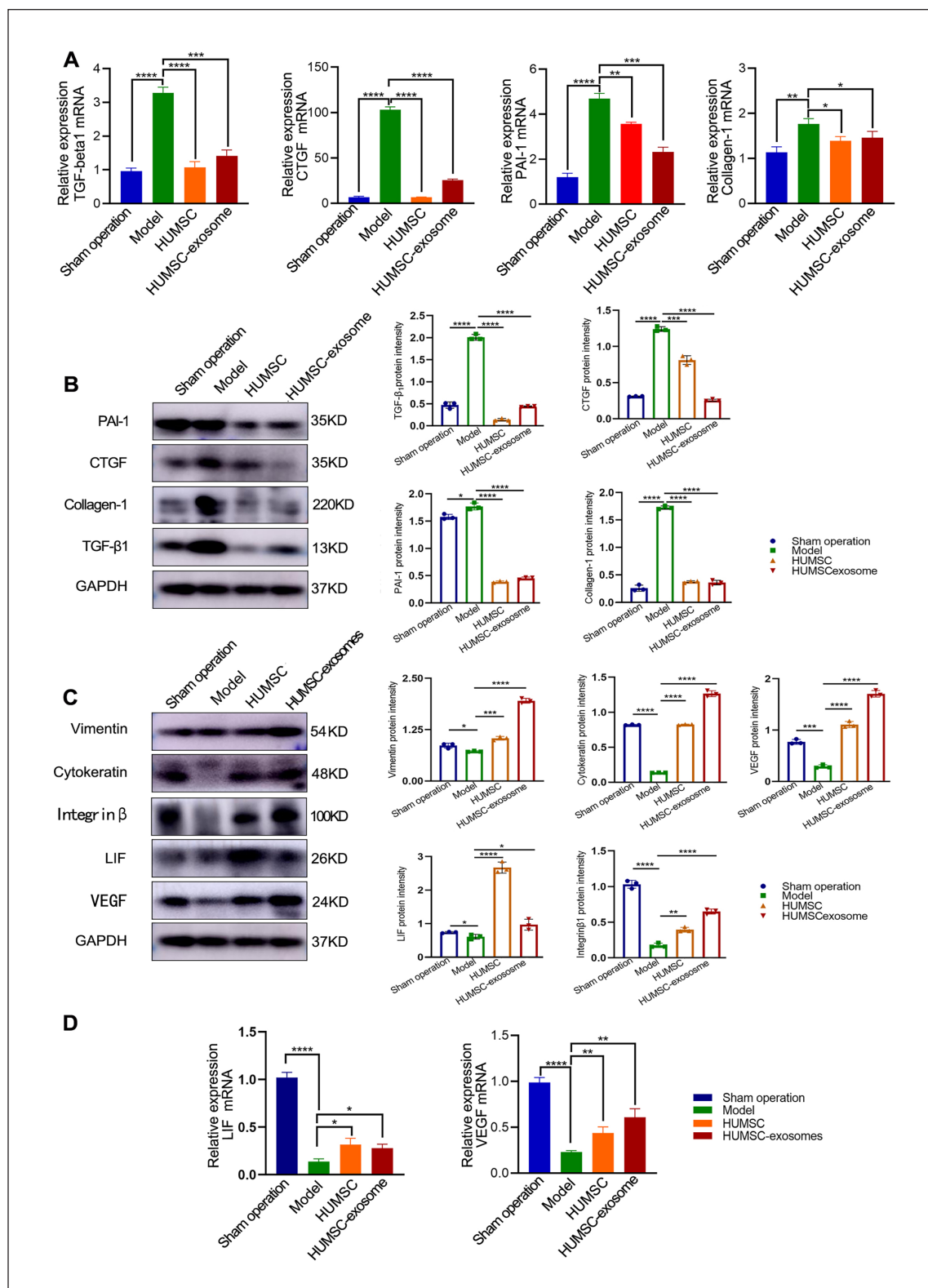


**Figure 9.** Protein and mRNA expression of markers for endometrial fibrosis and endometrial receptivity with Western blotting (B, C) and qPCR (A, D) represent the sham operation group, model group, HUMSC group, and HUMSC-exosome group, respectively. Bars represented mean  $\pm$  SD. HUMSC: human umbilical cord mesenchymal stem cell; qPCR: quantitative polymerase chain reaction; TGF- $\beta_1$ : transforming growth factor- $\beta_1$ ; CTGF: connective tissue growth factor; PAI-I: plasminogen activator inhibitor I; GAPDH: glyceraldehyde 3-phosphate dehydrogenase; LIF: leukemia inhibitory factor. \* $P < 0.05$ ; \*\* $P < 0.01$ ; \*\*\* $P < 0.001$ ; \*\*\*\* $P < 0.0001$ , compared with the model group;  $n = 3$ .

was obviously much greater than that in the control group ( $P < 0.05$  and  $<0.05$ , respectively) (Fig. 10C and D).

TGF- $\beta_1$  is recognized as one of the most important regulators of endometrial fibrosis. To investigate whether HUMSC and HUMSC-exosome attenuated endometrial fibrosis by inhibiting the TGF- $\beta_1$ /smad2/3 signaling pathway, we examined the expression of TGF- $\beta_1$ , smad2/3, and phosphorylated Smad2/3 (p-smad2/3) in HESCs by Western blotting (Fig. 10E). Compared with the control group, the protein expression levels of TGF- $\beta_1$ , smad2/3, and p-smad2/3 were significantly decreased in the HUMSC-exosome and HUMSC groups ( $P < 0.01$ ,  $<0.001$ , and  $<0.0001$ , respectively). Moreover, the expression of other fibrosis factors (PAI-1, CTGF, and collagen I) was also significantly decreased compared with that in the control group (Fig. 10F). In summary, our results suggested that HUMSC-exosome and HUMSC suppressed the TGF- $\beta_1$ /Smad2/3 signaling pathway in HESC fibrosis. Furthermore, the inhibition of fibrosis-related proteins, such as p-smad3, CTGF, and TGF- $\beta_1$ , was more potent in the HUMSC-exosome group.

## Discussion

In our work, a rat model of thin endometrium was successfully established by using ethanol foam, and high-quality HUMSC-exosome were obtained by pretreating HUMSC with TGF- $\beta_1$ . The results showed that not only the thickness of the endometrium, the number of glands, and subendometrial microangiogenesis were obviously increased but also the level of inhibition of endometrial fibrosis, molecular markers of endometrial receptivity, and the pregnancy rate were significantly improved.

In terms of modeling, an ethanol foaming agent with strong absorption and weak liquidity was injected into one side of the uterus, which can prevent the uterus from being clamped by hemostatic forceps and cause uterine cavity stenosis and water accumulation. It should be noted that this is different from traditional methods, which use silk thread or hemostatic forceps to clamp both ends of the uterus and inject absolute ethanol to establish a thin endometrial model.

The production of endometrial injury models has been reported in rats<sup>26</sup>, mice<sup>27</sup>, New Zealand rabbits<sup>28</sup>, and so on. The methods applied include mechanical injury and infection, thermal damage, chemical damage, optical damage, and so on. Thin endometrial models are mostly established by intrauterine injection of 95% ethanol in SD rats, first proposed by Zhao et al.<sup>29,30</sup> This modeling method involves clamping one end of the rat's uterus and then injecting 95% ethanol to chemically damage the endometrium, but the survival rate after modeling is only 70% and it often results in rat uterine hydrops and severe abdominal cavity adhesions. The modeling method we adopted did not require the use of hemostatic forceps to clamp the uterus, thus avoiding uterine hydrops and abdominal adhesions caused by surgery. Meanwhile, our method provides a good foundation for

subsequent pregnancy tests and is closer to the pathological condition of human thin endometrium.

In this experiment, we obtained the cell supernatant after treatment of HUMSC with TGF- $\beta_1$ . The purity of the exosomes extracted by speed ultracentrifugation was significantly higher than that obtained from untreated HUMSC, the morphology of the exosomes was well maintained with few impurities under electron microscopy, and the exosomes could be well phagocytosed by HESCs. We observed that some exosomes labeled with PKH26 entered the cytoplasm and were phagocytosed.

Several previous studies have shown that certain chemicals can effectively promote the release of exosomes and optimize the therapeutic effect<sup>31,32</sup>. Liao et al.<sup>33</sup> found that metformin promoted the release of extracellular nanocapsules of MSC origin to promote disk degeneration repair. TGF- $\beta$  (mainly the TGF- $\beta_1$  isoform) regulates various cellular activities, including cell proliferation, differentiation, migration, apoptosis, inflammatory and immune responses, angiogenesis, fibrosis, and tissue repair<sup>34–36</sup>. Low concentrations of TGF- $\beta_1$  stimulate stem cell proliferation<sup>37</sup>. Thus, in our work, HUMSC were stimulated with TGF- $\beta_1$  (10 ng/ml) to promote exosomes secretion, to obtain high-quality exosome, and to enhance HESCs proliferation. In addition, exosomes are mixed with gel. The main component of the gel is cross-linked sodium hyaluronate, which has good biocompatibility, physical rheological properties, and unique biological effects, stabilizing the structure of exosomes and prolonging their action in the uterine cavity.

Cytokeratin, which is closely related to the proliferation of epithelial cells, mainly maintains the integrity and continuity of epithelial tissue. Vimentin constitutes the cytoskeleton and maintains the integrity of the cytoskeleton<sup>38</sup>. After treatment, the histological and protein expression of cytokeratin and vimentin was significantly increased in the HUMSC and HUMSC-exosome groups compared with the model group. This indicated that the endothelium was repaired and increased in thickness in the treated group.

CTGF has been found to induce fibroblast proliferation and secretion of extracellular matrix (ECM), which is closely related to the development of fibrosis in many tissues and organs. PAI-1 (also known as SERPINE1) is an essential factor involved in the regulation of the physiological balance between thrombosis and fibrinolysis, and it plays important roles in cell migration, adhesion, and tissue remodeling<sup>39,40</sup>. Collagen I is also a marker of fibrosis. In our study, the mRNA and protein expression of CTGF, PAI-1, and collagen I was obviously decreased in the HUMSC and HUMSC-exosome groups.

VEGF is an important regulator of vascular morphogenesis, promoting the growth of vascular endothelial cells and inducing vascular proliferation<sup>41</sup>. CD34+ cells have been associated with therapeutic angiogenesis in response to ischemia<sup>42</sup>. Subendometrial microangiogenesis plays a key role in the improvement of endometrial receptivity for successful

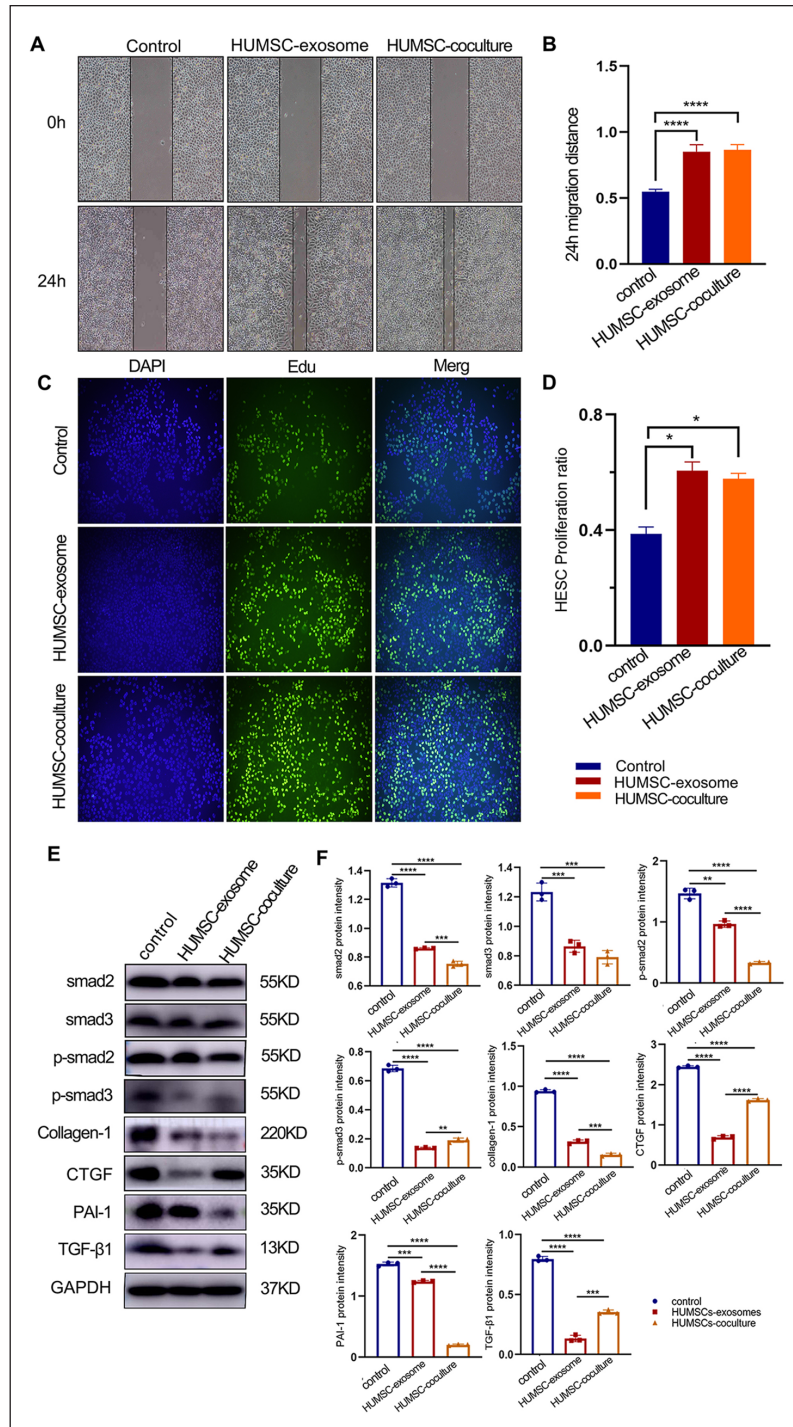


**Figure 10.** (A) HESCs scratch test with HUMSC-exosome and HUMSC-coculture. (B) The histogram confirmed that the migration potential of the HUMSC-exosome and HUMSC-coculture groups at 24 h was greater than that of the control group ( $P < 0.0001$ , respectively). (C) EdU was applied to detect DNA replication (green fluorescence) after HUMSC-exosome culture and HUMSC-coculture with HESCs for 24 h. (D) The histogram showed proliferation ratio of HESCs in the control, HUMSC-exosome, and HUMSC groups. The DNA replication of HESCs in the HUMSC group and HUMSC-exosome group was much higher than that in the control group ( $P < 0.05$ , respectively). (E) As evidenced by the Western blotting images and the quantitative data, HUMSC and HUMSC-exosome group inhibited the protein levels of p-smad2/3 and smad2/3 in HESCs pretreated with TGF- $\beta_1$  (10 ng/ml) for 48 h; in addition, their downregulation led to lower expression of fibrosis-related factors (PAI-1, CTGF, collagen I, and  $\alpha$ -SMA). (F) Data are presented as mean  $\pm$  SD. HESCs: human endometrial stromal cell; HUMSC: human umbilical cord mesenchymal stemcell; EdU: 5-ethynyl-2'-deoxyuridine; TGF- $\beta_1$ : transforming growth factor- $\beta_1$ ; CTGF: connective tissue growth factor; PAI-1: plasminogen activator inhibitor 1;  $\alpha$ -SMA: alpha smooth muscle actin; DAPI: 4',6-diamidino-2-phenylindole; GAPDH: glyceraldehyde 3-phosphate dehydrogenase. \* $P < 0.05$ ; \*\* $P < 0.01$ ; \*\*\* $P < 0.001$ ; \*\*\*\* $P < 0.0001$  versus the control group,  $n = 3$ .

embryo implantation<sup>43</sup>. Numerous studies have investigated the regulation of subendometrial microangiogenesis and shown that microangiogenesis is regulated by VEGF, which is expressed in the human endometrium<sup>44</sup>. The expression of VEGF and CD34 was significantly higher in the HUMSC and HUMSC-exosome groups.

In our study, the histological and protein expression levels of integrin  $\beta_3$  and LIF were significantly reduced in the rat model of thin endometrium without HUMSC or HUMSC-exosome therapy, and the HUMSC/HUMSC-exosome groups had almost normal expression of integrin  $\beta_3$  and LIF. The integrin  $\beta_3$  and LIF, as important regulators and markers of endometrial receptivity, play a vital role in embryo implantation<sup>45</sup>. Integrin  $\beta_3$  plays an important role in embryo attachment, and LIF, which is thought to play a crucial role in implantation, is expressed in blastocysts and the endometrium. In our pregnancy trial, pregnancy rates were greatly improved in the treated groups compared with the model group, which is a strong indication of the effectiveness of HUMSC/HUMSC-exosome treatment.

Consistent with the *in vivo* and *in vitro* study results, the treatment of HESCs with HUMSC or HUMSC-exosome significantly reduced TGF- $\beta_1$  mRNA and protein expression, as well as the phosphorylation of Smad2/3. In addition, the mRNA and protein expression of CTGF and PAI-1 were also reduced. TGF- $\beta_1$  has been shown to be a strong inducer of CTGF and PAI-1 in animal models of cardiac remodeling<sup>39</sup>. Smad2/3 is a major downstream target of TGF- $\beta_1$  and is involved in the expression of CTGF and PAI-1 in different cell types and tissues<sup>46</sup>. Our results suggested that TGF- $\beta_1$ /Smad2/3 signaling may be involved in the inhibitory effect of HUMSC or HUMSC-exosome on TGF- $\beta_1$ -induced high expression of PAI-1 and CTGF, which are related to fibrosis.

Recently, MSC have emerged as a promising approach for tissue repairing and regeneration<sup>47</sup>. However, focus on the therapeutic role of MSC of regenerative medicine has shifted to their activity through paracrine secretion instead of differentiation into functional cells. MSC induce regeneration through paracrine secretion to rescue injured cells, reduce tissue damage, and ultimately accelerate organ repair<sup>48,49</sup>. MSC release great amount of extracellular vesicles (mainly exosomes) which participate in tissue regeneration through delivering information to damaged cells or tissues and exert biological activity similar to the MSC<sup>50</sup>. Our results also confirmed these points. Exosomes can be readily isolated from MSC, and MSC-exosomes are now known to have significant therapeutic benefits in a series of animal disease models. In a sense, these effects have been clearly demonstrated to be of equal potency to those observed with whole-cell MSC administration. Consequently, exosomes could be an effective, safe, and inexpensive approach in cell-free regenerative medicine and promising to become a suitable alternative instead of MSC.

## Author Contributions

Shengning Zhang performed all the experiments and participated in writing the manuscript. Dongmei Wang, Fang Yang, Yanjun Shen, and Dong Li assisted with the experiments. Dong Li and Xiaohui Deng conceived the project, analyzed the data, and actively participated in manuscript writing.

## Ethical Approval

This study was approved by the ethics committee of Qilu Hospital of Shandong University Shandong Province, China (approval No. 2018207).

## Statement of Human and Animal Rights

All procedures in this study were conducted in accordance with the Ethical Committee on Animal Experiment of Shandong University Qilu Hospital (approval No. DULL-2020-044)-approved protocols.

## Statement of Informed Consent

Written informed consent was obtained from each umbilical cord donor.

## Declaration of Conflicting Interests


The author(s) declared no potential conflicts of interest with respect to the research, authorship, and/or publication of this article.

## Funding

The author(s) disclosed receipt of the following financial support for the research, authorship, and/or publication of this article: This work was supported by Department of Science & Technology of Shandong Province (ZR2020MH063).

## ORCID iDs

Dong Li  <https://orcid.org/0000-0002-6496-4605>

Xiaohui Deng  <https://orcid.org/0000-0001-8769-4014>

## Supplemental Material

Supplemental material for this article is available online.

## References

1. Craciunas L, Gallos I, Chu J, Bourne T, Quenby S, Brosens JJ, Coomarasamy A. Conventional and modern markers of endometrial receptivity: a systematic review and meta-analysis. *Hum Reprod Update*. 2019;25(2):202–23.
2. Izquierdo A, de la Fuente L, Spies K, Rayward J, López L, Lora D, Galindo A. Endometrial scratch vs no intervention in egg donation cycles: the ENDOSCRATCH trial protocol. *BMC Pregnancy Childbirth*. 2020;20(1):333.
3. Jimenez PT, Schon SB, Odem RR, Ratts VS, Jungheim ES. A retrospective cross-sectional study: fresh cycle endometrial thickness is a sensitive predictor of inadequate endometrial thickness in frozen embryo transfer cycles. *Reprod Biol Endocrinol*. 2013;11:35.



4. Silva Martins R, Helio Oliani A, Vaz Oliani D, Martinez de Oliveira J. Subendometrial resistance and pulsatility index assessment of endometrial receptivity in assisted reproductive technology cycles. *Reprod Biol Endocrinol*. 2019;17(1):62.
5. Zhang W, Li X, Li H, Lu X, Chen J, Li L, Sun X, Xu C. 17 $\beta$ -estradiol promotes bone marrow mesenchymal stem cell migration mediated by chemokine upregulation. *Biochem Biophys Res Commun*. 2020;530(2):381–88.
6. Zhu X, Péault B, Yan G, Sun H, Hu Y, Ding L. Stem cells and endometrial regeneration: from basic research to clinical trial. *Curr Stem Cell Res Ther*. 2019;14(4):293–304.
7. Azizi R, Aghebati-Maleki L, Nouri M, Marofi F, Negargar S, Yousefi M. Stem cell therapy in Asherman syndrome and thin endometrium: stem cell- based therapy. *Biomed Pharmacother*. 2018;102:333–43.
8. Liu Y, Zhang Z, Yang F, Wang H, Liang S, Wang H, Yang J, Lin J. The role of endometrial stem cells in the pathogenesis of endometriosis and their application to its early diagnosis. *Biol Reprod*. 2020;102(6):1153–59.
9. Xin L, Lin X, Pan Y, Zheng X, Shi L, Zhang Y, Ma L, Gao C, Zhang S. A collagen scaffold loaded with human umbilical cord-derived mesenchymal stem cells facilitates endometrial regeneration and restores fertility. *Acta Biomater*. 2019;92:160–71.
10. de Miguel-Gómez L, Ferrero H, López-Martínez S, Campo H, López-Pérez N, Faus A, Hervás D, Santamaría X, Pellicer A, Cervelló I. Stem cell paracrine actions in tissue regeneration and potential therapeutic effect in human endometrium: a retrospective study. *BJOG*. 2020;127(5):551–60.
11. da Silva Meirelles L, Caplan AI, Nardi NB. In search of the in vivo identity of mesenchymal stem cells. *Stem Cells*. 2008;26(9):2287–99.
12. Noiseux N, Gneccchi M, Lopez- Ilasaca M, Zhang L, Solomon SD, Deb A, Dzau VJ, Pratt RE. Mesenchymal stem cells over-expressing Akt dramatically repair infarcted myocardium and improve cardiac function despite infrequent cellular fusion or differentiation. *Mol Ther*. 2006;14(6):840–50.
13. Iso Y, Spees JL, Serrano C, Bakondi B, Pochampally R, Song YH, Sobel BE, Delafontaine P, Prockop DJ. Multipotent human stromal cells improve cardiac function after myocardial infarction in mice without long-term engraftment. *Biochem Biophys Res Commun*. 2007;354(3):700–706.
14. Eiró N, Sendon-Lago J, Seoane S, Bermúdez MA, Lamelas ML, Garcia-Caballero T, Schneider J, Perez-Fernandez R, Vizoso FJ. Potential therapeutic effect of the secretome from human uterine cervical stem cells against both cancer and stromal cells compared with adipose tissue stem cells. *Oncotarget*. 2014;5(21):10692–10708.
15. Bermudez MA, Sendon-Lago J, Eiro N, Treviño M, Gonzalez F, Yebra-Pimentel E, Giraldez MJ, Macia M, Lamelas ML, Saa J, Vizoso F, et al. Corneal epithelial wound healing and bactericidal effect of conditioned medium from human uterine cervical stem cells. *Invest Ophthalmol Vis Sci*. 2015;56(2):983–92.
16. Bermudez MA, Sendon-Lago J, Seoane S, Eiro N, Gonzalez F, Saa J, Vizoso F, Perez-Fernandez R. Anti-inflammatory effect of conditioned medium from human uterine cervical stem cells in uveitis. *Exp Eye Res*. 2016;149:84–92.
17. Osugi M, Katagiri W, Yoshimi R, Inukai T, Hibi H, Ueda M. Conditioned media from mesenchymal stem cells enhanced bone regeneration in rat calvarial bone defects. *Tissue Eng Part A*. 2012;18(13–14):1479–89.
18. Collino F, Pomatto M, Bruno S, Lindoso RS, Tapparo M, Sicheng W, Quesenberry P, Camussi G. Exosome and microvesicle-enriched fractions isolated from mesenchymal stem cells by gradient separation showed different molecular signatures and functions on renal tubular epithelial cells. *Stem Cell Rev Rep*. 2017;13(2):226–43.
19. Jafari D, Malih S, Eini M, Jafari R, Gholipourmalekabadi M, Sadeghizadeh M, Samadikuchaksaraei A. Improvement, scaling-up, and downstream analysis of exosome production. *Crit Rev Biotechnol*. 2020;40(8):1098–1112.
20. Meng XM, Chung AC, Lan HY. Role of the TGF- $\beta$ /BMP-7/Smad pathways in renal diseases. *Clin Sci (Lond)*. 2013;124(4):243–54.
21. Qi L, Wang R, Shi Q, Yuan M, Jin M, Li D. Umbilical cord mesenchymal stem cell conditioned medium restored the expression of collagen II and aggrecan in nucleus pulposus mesenchymal stem cells exposed to high glucose. *J Bone Miner Metab*. 2019;37(3):455–66.
22. Sun L, Li D, Song K, Wei J, Yao S, Li Z, Su X, Ju X, Chao L, Deng X, Kong B, et al. Exosomes derived from human umbilical cord mesenchymal stem cells protect against cisplatin-induced ovarian granulosa cell stress and apoptosis in vitro. *Sci Rep*. 2017;7(1):2552.
23. Zhang HS, Yang AJ, Liu S. Identifying the most stable state of a foam sclerosant for foam sclerotherapy. *Dermatol Surg*. 2020;46(10):e66–70.
24. Hanshu Z, Shaohua L, Anwei C. A novel compound sclerosant: polidocanol-bleomycin foam. *Dermatol Surg*. 2020;46(12):1712–14.
25. Nicola NA, Babon JJ. Leukemia inhibitory factor (LIF). *Cytokine Growth Factor Rev*. 2015;26(5):533–44.
26. Guney M, Oral B, Karahan N, Mungan T. Protective effect of caffeic acid phenethyl ester (CAPE) on fluoride-induced oxidative stress and apoptosis in rat endometrium. *Environ Toxicol Pharmacol*. 2007;24(2):86–91.
27. Alawadhi F, Du H, Cakmak H, Taylor HS. Bone Marrow-Derived Stem Cell (BMDSC) transplantation improves fertility in a murine model of Asherman's syndrome. *Plos One*. 2014;9(5):e96662.
28. Khrouf M, Morel O, Hafiz A, Chavatte-Palmer P, Fernandez H. Evaluation of the rabbit as an experimental model for human uterine synechia. *J Hum Reprod Sci*. 2012;5(2):175–80.
29. Zhao J, Zhang Q, Wang Y, Li Y. Uterine infusion with bone marrow mesenchymal stem cells improves endometrium thickness in a rat model of thin endometrium. *Reprod Sci*. 2015;22(2):181–88.
30. Zhao J, Yan Y, Huang X, Lun-Quan S, Li Y. Therapeutic effects of VEGF gene-transfected BMSCs transplantation on thin endometrium in the rat model. *Stem Cells Int*. 2018;2018:3069741.
31. Li R, He Y, Zhu Y, Jiang L, Zhang S, Qin J, Wu Q, Dai W, Shen S, Pang Z, Wang J. Route to rheumatoid arthritis by macrophage-derived microvesicle-coated nanoparticles. *Nano Lett*. 2019;19(1):124–34.
32. Soraya H, Sani NA, Jabbari N, Rezaie J. Metformin increases exosome biogenesis and secretion in U87 MG human glioblastoma cells: a possible mechanism of therapeutic resistance. *Arch Med Res*. 2021;52(2):151–62.

33. Liao Z, Li S, Lu S, Liu H, Li G, Ma L, Luo R, Ke W, Wang B, Xiang Q, Song Y, et al. Metformin facilitates mesenchymal stem cell-derived extracellular nanovesicles release and optimizes therapeutic efficacy in intervertebral disc degeneration. *Biomaterials*. 2021;274:120850.
34. Pardali E, Goumans MJ, ten Dijke P. Signaling by members of the TGF-beta family in vascular morphogenesis and disease. *Trends Cell Biol*. 2010;20(9):556–67.
35. Morikawa M, Derynck R, Miyazono K. TGF- $\beta$  and the TGF- $\beta$  family: context-dependent roles in cell and tissue physiology. *Cold Spring Harb Perspect Biol*. 2016;8(5):a021873.
36. Lichtman MK, Otero-Vinas M, Falanga V. Transforming growth factor beta (TGF- $\beta$ ) isoforms in wound healing and fibrosis. *Wound Repair Regen*. 2016;24(2):215–22.
37. Zhang Q, Fu L, Liang Y, Guo Z, Wang L, Ma C, Wang H. Exosomes originating from MSCs stimulated with TGF- $\beta$  and IFN- $\gamma$  promote Treg differentiation. *J Cell Physiol*. 2018;233(9):6832–40.
38. Zhou ZQ, Chen Y, Chai M, Tao R, Lei YH, Jia YQ, Shu J, Ren J, Li G, Wei WX, Han YD, et al. Adipose extracellular matrix promotes skin wound healing by inducing the differentiation of adipose-derived stem cells into fibroblasts. *Int J Mol Med*. 2019;43(2):890–900.
39. Gifford CC, Tang J, Costello A, Khakoo NS, Nguyen TQ, Goldschmeding R, Higgins PJ, Samarakoon R. Negative regulators of TGF- $\beta$ 1 signaling in renal fibrosis; pathological mechanisms and novel therapeutic opportunities. *Clin Sci (Lond)*. 2021;135(2):275–303.
40. Samarakoon R, Goppelt-Strube M, Higgins PJ. Linking cell structure to gene regulation: signaling events and expression controls on the model genes PAI-1 and CTGF. *Cell Signal*. 2010;22(10):1413–19.
41. Peng L, Yin J, Wang S, Ge M, Han Z, Wang Y, Zhang M, Xie L, Li Y. TGF- $\beta$ 2/Smad3 signaling pathway activation through enhancing VEGF and CD34 ameliorates cerebral ischemia/reperfusion injury after isoflurane post-conditioning in rats. *Neurochem Res*. 2019;44(11):2606–18.
42. Prasad M, Corban MT, Henry TD, Dietz AB, Lerman LO, Lerman A. Promise of autologous CD34+ stem/progenitor cell therapy for treatment of cardiovascular disease. *Cardiovasc Res*. 2020;116(8):1424–33.
43. Karizbodagh MP, Rashidi B, Sahebkar A, Masoudifar A, Mirzaei H. Implantation window and angiogenesis. *J Cell Biochem*. 2017;118(12):4141–51.
44. Fraser HM, Wilson H, Silvestri A, Morris KD, Wiegand SJ. The role of vascular endothelial growth factor and estradiol in the regulation of endometrial angiogenesis and cell proliferation in the marmoset. *Endocrinology*. 2008;149(9):4413–20.
45. Hajipour H, Sambrani R, Ghorbani M, Mirzamohammadi Z, Nouri M. Sildenafil citrate-loaded targeted nanostructured lipid carrier enhances receptivity potential of endometrial cells via LIF and VEGF upregulation. *Naunyn Schmiedeberg Arch Pharmacol*. 2021;394(11):2323–31.
46. Lv Q, Wang J, Xu C, Huang X, Ruan Z, Dai Y. Pirfenidone alleviates pulmonary fibrosis in vit ro and in vivo through regulating Wnt/GSK-3 $\beta$ / $\beta$ -catenin and TGF- $\beta$ 1/Smad2/3 signaling pathways. *Mol Med*. 2020;26(1):49.
47. Fu X, Liu G, Halim A, Ju Y, Luo Q, Song AG. Mesenchymal stem cell migration and tissue repair. *Cells*. 2019;8(8):784.
48. Baraniak PR, McDevitt TC. Stem cell paracrine actions and tissue regeneration. *Regen Med*. 2010;5(1):121–43.
49. Veneruso V, Rossi F, Vilella A, Bena A, Forloni G, Veglianesi P. Stem cell paracrine effect and delivery strategies for spinal cord injury regeneration. *J Control Release*. 2019;300:141–53.
50. Keshtkar S, Azarpira N, Ghahremani MH. Mesenchymal stem cell-derived extracellular vesicles: novel frontiers in regenerative medicine. *Stem Cell Res Ther*. 2018;9(1):63.